Journal of Computational Mathematics, Vol.27, No.2-3, 2009, 196–214.

THE ELLIPSOID ARTIFICIAL BOUNDARY METHOD FOR THREE-DIMENSIONAL UNBOUNDED DOMAINS*

Hongying Huang
Information College, Zhejiang Ocean University, Zhoushan 316004, China
Email: huanghy@lsec.cc.ac.cn
Dehao Yu
LSEC, ICMSEC, Academy of Mathematics and System Sciences, Chinese Academy of Sciences, Beijing 100080, China
Email: ydh@lsec.cc.ac.cn

Abstract

The artificial boundary method is applied to solve three-dimensional exterior problems. Two kind of rotating ellipsoids are chosen as the artificial boundaries and the exact artificial boundary conditions are derived explicitly in terms of an infinite series. Then the well-posedness of the coupled variational problem is obtained. It is found that error estimates derived depend on the mesh size, truncation term and the location of the artificial boundary. Three numerical examples are presented to demonstrate the effectiveness and accuracy of the proposed method.

Mathematics subject classification: 65N38, 65N30.
Key words: Artificial boundary method, Exterior harmonic problem, Finite element method, Natural boundary reduction, Oblate ellipsoid, Prolate ellipsoid.

1. Introduction

Many problems in science and engineering lead to solving boundary value problems of partial differential equations in unbounded domains. The main difficulty in finding the numerical solutions of these problems is the unboundedness of the domain. In the 1970s, attempts have been made to apply the finite element method (FEM) [3] and the finite difference method (FDM) [11] to solve these problems numerically. However, the standard FEM and FDM are not effective in solving these problems. Later, Brebbia, Hsiao and Wendland developed the boundary element method (BEM), which can reduce the dimension of the computational domain and is suitable for solving problems in the unbounded domains. Then Zienkiewicz and Kelly [34], Brezzi and Johnson [6], Johnson and Nedelec [25], Han [18], Costabel and Stephan [35] suggested the coupling of FEM and BEM, which allows to combine the advantages of BEM in treating linear problems over unbounded domains with those of FEM in treating linear and nonlinear problems over the complicated bounded domains.

The artificial boundary method (including the coupling of FEM and BEM) [10, 12, 14, 15, 17, 26, 30] reduces the original problem in an unbounded domain to am equivalent problem in a bounded domain with some suitable boundary condition on the artificial boundary. The standard procedure of the method is described as follows. First, an artificial boundary Γ is introduced to divide the original (unbounded) domain $\Omega^c = \mathbb{R}^3 \backslash (\Omega \cup \partial\Omega)$ into two subregions, a bounded inner region and an unbounded outer one. Next, certain boundary condition must be

* Received December 16, 2007 / Revised version received May 10, 2008 / Accepted May 20, 2008 /

imposed on it. Lastly, the original problem is reduced to an equivalent one in the bounded region which is solved numerically. It is very important that how to design the suitable boundary condition on the artificial boundary and how to solve the coupled system. When the imposed boundary condition is exact and non-reflective and usually is expressed by the series in generalized sense, the method has been also called the DtN method by Keller [26,27] or the coupling of FEM and natural boundary element method (NBEM) by Yu [30].

Natural boundary reduction proposed by Feng and Yu [13] has advantages over the usual boundary reduction methods: the coupled bilinear form preserves automatically the symmetry and coerciveness of the original bilinear form, so not only the analysis of the discrete problem is simplified but also the optimal error estimates and the numerical stability are restored. These advantages make the coupling of FEM and natural boundary reduction natural and direct. Moreover, this coupling of FEM and NBEM [26,30,32] also permits us to combine the advantages of BEM for treating linear problems over unbounded domains and some problems with singularity with those of FEM. The coupled method was first applied to solve the elliptic problems in two-dimensional domain [32]. Later Du and Yu [8,9], Wu and Yu [27,29], Hu and Yu [21], Liu [28], Gatica [36] use the method to handle evolution equations, the problems over three-dimensional domains, nonlinear interface problems, the electromagnetic problems and nonlinear problem in incompressible elasticity, respectively.

For three-dimensional exterior problems, a spherical surface [27,29] is usually selected as the artificial boundary. However, for an cigar-shaped or flying saucer-shaped obstacles, a rotating ellipsoid boundary [22–24] is used as the artificial boundary. This turns out to be very efficient since it leads to a smaller computational domain, as shown in Fig. 1.1 and does not increase the computational complexity of the stiff matrix from boundary reduction using the rotating ellipsoid artificial boundary. On the other hand, an anisotropic exterior problem with the constant coefficients with the spherical artificial boundary can be reduced to an isotropic problem with the ellipsoid artificial boundary.

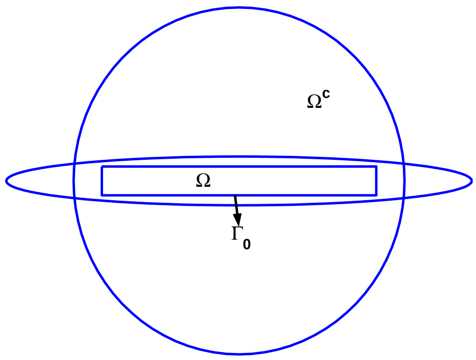

Fig. 1.1. Cross-section of cigar-shaped, ellipsoid and sphere.

Section 2 of this paper introduces two kind of rotating ellipsoids as the artificial boundaries and derives the exact artificial boundary conditions, which are expressed explicitly by the series. In Section 3, an equivalent coupled variational problem is given and the well-posedness of its continuous and discrete variational problem is obtained. In Section 4, error estimates which depend not only on the mesh size, but also on the term after truncating the series and the location of the artificial boundary [20,31] are discussed. Lastly, three numerical examples are presented to demonstrate the effectiveness and accuracy of the proposed method.

2. Exact Artificial Boundary Condition

Let $\Omega \subset \mathbb{R}^3$ be a cigar-shaped or flying saucer-shaped Lipschitz bounded domain including the coordinate origin, $\Omega^c = \mathbb{R}^3 \backslash (\Omega \cup \Gamma_0)$ and $\Gamma_0 = \partial\Omega$. Assume that the given functions f and g satisfy $g \in H^{1/2}(\Gamma_0)$ and $f \in L^2(\Omega^c)$, $supp(f) \subset \Omega^c$. Consider the following exterior Dirichlet problem:

$$\begin{cases} -\Delta u = f, & \text{in } \Omega^c, \\ u = g, & \text{on } \Gamma_0, \end{cases} \tag{2.1}$$

subject to the asymptotic conditions

$$u(x^1, x^2, x^3) = \mathcal{O}\left(\frac{1}{r}\right) \quad \text{as } r = \sqrt{x^1 + x^2 + x^3} \to \infty,$$
$$|\nabla u(x^1, x^2, x^3)| = \mathcal{O}\left(\frac{1}{r^2}\right) \quad \text{as } r = \sqrt{x^1 + x^2 + x^3} \to \infty.$$

The problem (2.1) is well-posed in $W_g^1(\Omega^c)$ [33], where

$$W_g^1(\Omega^c) = \left\{ v : \frac{v}{r}, \frac{\partial v}{\partial x^1}, \frac{\partial v}{\partial x^2}, \frac{\partial v}{\partial x^3} \in L^2(\Omega^c), v|_{\partial\Omega} = g \right\}.$$

Its norm and semi-norm are defined as

$$\|v\|_{W_g^1(\Omega^c)} = \left(\left\|\frac{v}{r}\right\|^2_{L^2(\Omega^c)} + \left\|\frac{\partial v}{\partial x^1}\right\|^2_{L^2(\Omega^c)} + \left\|\frac{\partial v}{\partial x^2}\right\|^2_{L^2(\Omega^c)} + \left\|\frac{\partial v}{\partial x^3}\right\|^2_{L^2(\Omega^c)} \right)^{\frac{1}{2}}$$
$$|v|_{W_g^1(\Omega^c)} = \left(\left\|\frac{\partial v}{\partial x^1}\right\|^2_{L^2(\Omega^c)} + \left\|\frac{\partial v}{\partial x^2}\right\|^2_{L^2(\Omega^c)} + \left\|\frac{\partial v}{\partial x^3}\right\|^2_{L^2(\Omega^c)} \right)^{\frac{1}{2}},$$

respectively.

Introduce an artificial boundary Γ which divides Ω^c into two subregions: a bounded inner region Ω_1 and a unbounded outer region Ω_2 (Fig. 2.1 and Fig. 2.2) such that $\Omega_1 \cap \Omega_2 = \varnothing$, $\overline{\Omega_1} \cup \overline{\Omega_2} = \overline{\Omega^c}$, $\mathrm{supp}(f) \subset \Omega_1 \cup \Omega \cup \Gamma_0$.

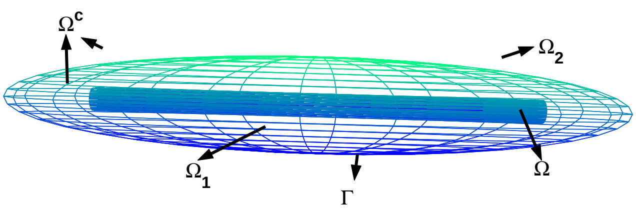

Fig. 2.1. prolate ellipsoid.

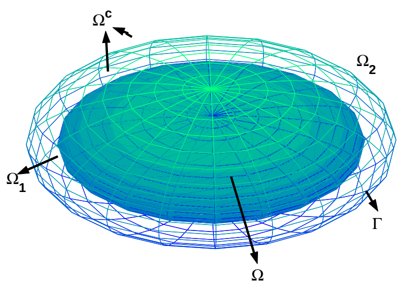

Fig. 2.2. oblate ellipsoid.

2.1. Prolate ellipsoid

When Ω is cigar-shaped, let the artificial boundary

$$\Gamma = \left\{(x_1, x_2, x_3) : x_1^2/b^2 + x_2^2/b^2 + x_3^2/a^2 = 1, a > b > 0\right\}$$

and its prolate ellipsoidal coordinate be $\Gamma = \{\, (\mu, \theta, \varphi) : \mu = \mu_1 > 0, \theta \in [0, \pi], \varphi \in [0, 2\pi) \,\}$. Let $f_0 = \sqrt{a^2 - b^2}$, $a = f_0 \cosh \mu_1$ and $b = f_0 \sinh \mu_1$. Take the following coordinate transformation:

$$\begin{cases} x_1 = f_0 \sinh \mu \sin \theta \cos \varphi, & \mu \geq \mu_1 > 0, \\ x_2 = f_0 \sinh \mu \sin \theta \sin \varphi, & \theta \in [0, \pi], \\ x_3 = f_0 \cosh \mu \cos \theta, & \varphi \in [0, 2\pi). \end{cases} \tag{2.2}$$

According to the boundary reduction theories [22, 24], if $u|_\Gamma = u(\mu_1, \theta, \varphi)$ is expanded to an absolutely and uniformly convergent series

$$u(\mu_1, \theta, \varphi) = \sum_{n=0}^{\infty} \sum_{m=-n}^{n} U_{nm} Y_{nm}(\theta, \varphi), \tag{2.3}$$

where

$$U_{nm} = \int_0^{\pi} \int_0^{2\pi} u(\mu_1, \theta, \varphi) Y_{nm}^*(\theta, \varphi) \sin \theta \, d\theta \, d\varphi,$$

Y_{nm} is the spherical harmonic functions and * denote the conjugate complex number, then the solution of the Laplace equation in the unbounded domain outside Γ is given by the series

$$u(\mu, \theta, \varphi) = \sum_{n=0}^{\infty} \sum_{m=-n}^{n} \frac{Q_n^m(\cosh \mu)}{Q_n^m(\cosh \mu_1)} U_{nm} Y_{nm}(\theta, \varphi), \qquad \mu \geq \mu_1 > 0, \tag{2.4}$$

which is convergent to the boundary value $u(\mu_1, \theta, \varphi)$. Here, the $Q_n^m(x)$ denote the second kind associated Legendre functions. Its normal derivative of the solution (2.4) on Γ (point to Ω_1) is

$$\frac{\partial u}{\partial \mathbf{n}} = -\frac{1}{f_0 \sqrt{\cosh^2 \mu_1 - \cos^2 \theta}} \sum_{n=0}^{\infty} \sum_{m=-n}^{n} \frac{dQ_n^m(\cosh \mu_1)/d\mu}{Q_n^m(\cosh \mu_1)} U_{nm} Y_{nm} \doteq \mathcal{K} u|_\Gamma. \tag{2.5}$$

2.2. Oblate ellipsoid

When Ω is flying saucer-shaped, let the artificial boundary

$$\Gamma = \left\{(x_1, x_2, x_3) : x_1^2/a^2 + x_2^2/a^2 + x_3^2/b^2 = 1, a > b > 0\right\}$$

and its oblate ellipsoidal coordinate be $\Gamma = \{\, (\mu, \theta, \varphi) : \mu = \mu_1 > 0, \theta \in [0, \pi], \varphi \in [0, 2\pi) \,\}$. Let $f_0 = \sqrt{a^2 - b^2}$, $a = f_0 \cosh \mu_1$ and $b = f_0 \sinh \mu_1$. Take the following coordinate transformation

$$\begin{cases} x_1 = f_0 \cosh \mu \sin \theta \cos \varphi, & \mu \geq \mu_1 > 0, \\ x_2 = f_0 \cosh \mu \sin \theta \sin \varphi, & \theta \in [0, \pi], \\ x_3 = f_0 \sinh \mu \cos \theta, & \varphi \in [0, 2\pi), \end{cases} \tag{2.6}$$

Through the oblate coordinate transformation, the Laplace operator becomes

$$\begin{aligned} \Delta u = & \frac{1}{f_0^2(\cosh^2 \mu - \sin^2 \theta)} \left\{ \frac{1}{\cosh \mu} \frac{\partial}{\partial \mu} \left(\cosh \mu \frac{\partial u}{\partial \mu} \right) \right. \\ & \left. + \frac{1}{\sin \theta} \frac{\partial}{\partial \theta} \Big(\sin \theta \frac{\partial u}{\partial \theta} \Big) + \Big(\frac{1}{\sin^2 \theta} - \frac{1}{\cosh^2 \mu} \Big) \frac{\partial^2 u}{\partial \varphi^2} \right\}. \end{aligned} \tag{2.7}$$

Using the method of separation of variables, the general form of the solution of the exterior harmonic equation is

$$u(\mu,\theta,\varphi)=\sum_{n=0}^{\infty}\sum_{m=-n}^{n}\sqrt{\frac{(n-m)!}{(n+m)!}}A_{nm}T_n^m(\sinh\mu)Y_{nm}(\theta,\varphi),$$

where, A_{nm} are arbitrary constants independent of μ, θ and φ,

$$T_n^m(x)=i\exp\Big(\frac{i\pi n}{2}\Big)Q_n^m(ix),\quad i^2=-1. \tag{2.8}$$

If $u|_\Gamma=u(\mu_1,\theta,\varphi)$ is expanded to an absolutely and uniformly convergent series

$$u(\mu_1,\theta,\varphi)=\sum_{n=0}^{\infty}\sum_{m=-n}^{n}U_{nm}Y_{nm}(\theta,\varphi), \tag{2.9}$$

where

$$U_{nm}=\int_0^{\pi}\int_0^{2\pi}u(\mu_1,\theta,\varphi)Y_{nm}^*(\theta,\varphi)\sin\theta\,d\theta\,d\varphi.$$

The method of separation of variables implies that the solution of the Laplace equation in the unbounded domain outside Γ is given by the series

$$u(\mu,\theta,\varphi)=\sum_{n=0}^{\infty}\sum_{m=-n}^{n}\frac{T_n^m(\sinh\mu)}{T_n^m(\sinh\mu_1)}U_{nm}Y_{nm}(\theta,\varphi),\quad \mu\ge\mu_1>0, \tag{2.10}$$

which is convergent to the boundary value $u(\mu_1,\theta,\varphi)$ and the normal derivative of the solution on Γ (pointed to Ω_1) is

$$\frac{\partial u}{\partial\mathbf{n}}|_\Gamma=\frac{-1}{f_0\sqrt{\cosh^2\mu_1-\sin^2\theta}}\sum_{n=0}^{\infty}\sum_{m=-n}^{n}\frac{dT_n^m(\sinh\mu_1)/d\mu}{T_n^m(\sinh\mu_1)}U_{nm}Y_{nm}\doteq\mathcal{K}u_1. \tag{2.11}$$

The formulas (2.5) and (2.11) are both the exact artificial boundary conditions. $\mathcal{K}$ is the natural integral operator [32], also is called the Steklov-Poincaré operator or DtN operator.

3. Coupled Variational Problem and Well-posedness

The variational form of the problem (2.1) is: Find $u\in W_g^1(\Omega^c)$ such that

$$\int_{\Omega^c}\nabla u\cdot\nabla v\,d\mathbf{x}=\int_{\Omega_1}f\,v\,d\mathbf{x},\quad \forall\,v\in\big\{\,v\in W_0^1(\Omega^c):v|_{\Gamma_0}=0\,\big\}, \tag{3.1}$$

where $d\mathbf{x}=dx_1\,dx_2\,dx_3$ is volume element. Define

$$D_k(u,v)=\int_{\Omega_k}\nabla u\nabla v\,d\mathbf{x},\quad k=1,2,$$

and

$$\hat{D}(\gamma u,\gamma v)=\int_\Gamma\frac{\partial u}{\partial\mathbf{n}}v\,dS,\quad \gamma u=u|_\Gamma.$$

The Green formula in the unbounded domain satisfy

$$\int_{\Omega^c}\nabla u\cdot\nabla v\,d\mathbf{x}=D_1(u,v)+\int_\Gamma\frac{\partial u}{\partial\mathbf{n}}v\,dS=D_1(u,v)+\hat{D}(\gamma u,\gamma v). \tag{3.2}$$

Let

$$V_g(\Omega_1) = \{\, v : v \in H^1(\Omega_1), v|_{\Gamma_0} = g \,\} \qquad V_0(\Omega_1) = \{\, v : v \in H^1(\Omega_1), v|_{\Gamma_0} = 0 \,\}.$$

Thus, the equivalent variational problem of the original problem is : Find $u \in V_g(\Omega_1)$ such that

$$D_1(u, v) + \hat{D}(\gamma u, \gamma v) = \int_{\Omega_1} f\, v\, d\mathbf{x}, \quad \forall\, v \in V_0(\Omega_1). \tag{3.3}$$

When $\mu \geq \mu_1 > 0$, set

$$Q_{nm}(\mu_1, \mu) = \begin{cases} \dfrac{Q_n^m(\cosh\mu)}{Q_n^m(\cosh\mu_1)}, & \text{as } \Gamma \text{ is prolate ellipsoid,} \\ \dfrac{T_n^m(\sinh\mu)}{T_n^m(\sinh\mu_1)}, & \text{as } \Gamma \text{ is oblate ellipsoid.} \end{cases}$$

$$T_{nm}(\mu) = \begin{cases} -\dfrac{dQ_n^m(\cosh\mu)/d\mu}{Q_n^m(\cosh\mu)} \sinh\mu, & \text{as } \Gamma \text{ is prolate ellipsoid,} \\ -\dfrac{dT_n^m(\sinh\mu)/d\mu}{T_n^m(\sinh\mu)} \cosh\mu, & \text{as } \Gamma \text{ is oblate ellipsoid.} \end{cases}$$

By the above analysis, we have

$$\hat{D}(\gamma u, \gamma v) = f_0 \sum_{n=0}^{\infty} \sum_{m=-n}^{n} T_{nm}(\mu_1) V_{nm}^* U_{nm}. \tag{3.4}$$

Let

$$\hat{D}_N(\gamma u, \gamma v) = f_0 \sum_{n=0}^{N} \sum_{m=-n}^{n} T_{nm}(\mu_1) V_{nm}^* U_{nm}, \tag{3.5}$$

where U_{nm} and V_{nm} are the generalized Fourier coefficients of γu and γv with respect to $Y_{nm}(\theta, \varphi)$.

In actual computations, we solve the following variational problem: Find $u^N \in V_g(\Omega_1)$ such that

$$D_1(u^N, v) + \hat{D}_N(\gamma u^N, \gamma v) = \int_{\Omega_1} f\, v\, d\mathbf{x}, \quad \forall\, v \in V_0(\Omega_1). \tag{3.6}$$

In order to discuss the well-posedness of the variational problems, we first give the properties of the second kind associated Legendre functions.

Lemma 3.1. *If $\mu > \mu_1 > 0$, then $Q_{nm}(\mu_1, \mu)$ and $T_{nm}(\mu)$ satisfy the following properties:*

$$\left(\frac{\sinh\mu_1}{\sinh\mu}\right)^{n+1} < Q_{nm}(\mu_1, \mu) < \left(\frac{\cosh\mu_1}{\cosh\mu}\right)^{n+1}, \tag{3.7}$$

$$(n+1)\sinh\mu < T_{nm}(\mu) < (n+1)\cosh\mu. \tag{3.8}$$

Proof. 1). The integral expression of $Q_n^m(x)$ gives [1]:

$$Q_n^m(x) = (-1)^m \frac{n!}{(n-m)!} \int_0^{\infty} \frac{\cosh mt}{\left(x + \sqrt{x^2 - 1}\cosh t\right)^{n+1}}\, dt, \tag{3.9}$$

which implies that

$$\frac{Q_n^m(\cosh\mu)}{Q_n^m(\cosh\mu_1)} = \frac{\displaystyle\int_0^\infty \frac{\cosh mt}{(\cosh\mu+\sinh\mu\cosh t)^{n+1}}\,dt}{\displaystyle\int_0^\infty \frac{\cosh mt}{(\cosh\mu_1+\sinh\mu_1\cosh t)^{n+1}}\,dt}.$$

Also, $\sinh(\mu_1-\mu)<0$ satisfies

$$\frac{\sinh\mu_1}{\sinh\mu} < \frac{\cosh\mu_1+\sinh\mu_1\cosh t}{\cosh\mu+\sinh\mu\cosh t} < \frac{\cosh\mu_1}{\cosh\mu}.$$

namely,

$$\left(\frac{\sinh\mu_1}{\sinh\mu}\right)^{n+1} < \frac{\displaystyle\int_0^\infty \frac{\cosh mt}{(\cosh\mu+\sinh\mu\cosh t)^{n+1}}\,dt}{\displaystyle\int_0^\infty \frac{\cosh mt}{(\cosh\mu_1+\sinh\mu_1\cosh t)^{n+1}}\,dt} < \left(\frac{\cosh\mu_1}{\cosh\mu}\right)^{n+1}.$$

Thus, we obtain

$$\left(\frac{\sinh\mu_1}{\sinh\mu}\right)^{n+1} < \frac{Q_n^m(\cosh\mu)}{Q_n^m(\cosh\mu_1)} < \left(\frac{\cosh\mu_1}{\cosh\mu}\right)^{n+1}.$$

On the other hand, the formula (3.9) implies that the integral expression of $T_n^m(\sinh\mu)$ is

$$T_n^m(\sinh\mu) = \frac{(-1)^m n!}{i^n(n-m)!}\exp\left(\frac{i\pi n}{2}\right)\int_0^\infty \frac{\cosh mt}{(\sinh\mu+\cosh\mu\cosh t)^{n+1}}\,dt. \tag{3.10}$$

For the same reason above, we have

$$\left(\frac{\sinh\mu_1}{\sinh\mu}\right)^{n+1} < \frac{T_n^m(\sinh\mu)}{T_n^m(\sinh\mu_1)} < \left(\frac{\cosh\mu_1}{\cosh\mu}\right)^{n+1}.$$

2). Let $x=\cosh\mu$. Recursive relations of $Q_n^m(x)$ [1] lead to

$$-\frac{\frac{d}{d\mu}Q_n^m(\cosh\mu)}{Q_n^m(\cosh\mu)}\sinh\mu = \frac{\frac{d}{dx}Q_n^m(x)}{Q_n^m(x)}(1-x^2) = (n+1)x-(n-m+1)\frac{Q_{n+1}^m(x)}{Q_n^m(x)}. \tag{3.11}$$

When $t\ge 0$, $\cosh\mu+\sinh\mu\cosh t > \cosh\mu+\sinh\mu$. The integral expression [1] of $Q_n^m(x)$ satisfies

$$\frac{(n+1-m)}{(n+1)}\frac{Q_{n+1}^m(x)}{Q_n^m(x)} = \frac{\displaystyle\int_0^\infty \frac{\cosh mt}{(\cosh\mu+\sinh\mu\cosh t)^{n+2}}\,dt}{\displaystyle\int_0^\infty \frac{\cosh mt}{(\cosh\mu+\sinh\mu\cosh t)^{n+1}}\,dt} < (x-\sqrt{x^2-1}).$$

The formula (3.11) yields

$$(n+1)\sqrt{x^2-1} < \frac{\frac{d}{dx}Q_n^m(x)}{Q_n^m(x)}(1-x^2) < (n+1)x,$$

namely,

$$(n+1)\sinh\mu \le -\frac{\frac{d}{d\mu}Q_n^m(\cosh\mu)}{Q_n^m(\cosh\mu)} \le (n+1)\cosh\mu.$$

Also, inserting $z = i\sinh\mu$ into (3.11) and (3.9) results in

$$-\frac{\dfrac{d}{d\mu}T_n^m(\sinh\mu)}{T_n^m(\sinh\mu)}\cosh\mu = -i\frac{\dfrac{d}{dz}Q_n^m(z)}{Q_n^m(z)}(1-z^2) = (n+1)(-iz) + (n-m+1)\frac{iQ_{n+1}^m(z)}{Q_n^m(z)},$$

and

$$0 \le \frac{iQ_{n+1}^m(z)}{Q_n^m(z)} = \frac{\displaystyle\int_0^\infty \frac{(n+1)\cosh mt}{(\sinh\mu+\cosh\mu\cosh t)^{n+2}}\,dt}{\displaystyle\int_0^\infty \frac{(n+1-m)\cosh mt}{(\sinh\mu+\cosh\mu\cosh t)^{n+1}}\,dt} \le \frac{(n+1)}{(n+1-m)}(\cosh\mu-\sinh\mu).$$

Thus, we have

$$(n+1)\sinh\mu \le -\frac{\dfrac{d}{d\mu}T_n^m(\sinh\mu)}{T_n^m(\sinh\mu)}\cosh\mu \le (n+1)\cosh\mu,$$

which proves the assertion (3.8). □

Remark 3.1. When $a/b = \cosh\mu_1/\sinh\mu_1 \to 1$, $\mu_1 \to \infty$. Let $a_1 = f_0\cosh\mu$ and use Lemma 3.1. Then we have $Q_{nm}(\mu_1,\mu) \to (a/a_1)^{n+1}$ and $T_{nm}(\mu_1) \to C(n+1)$. Therefore, when $\mu_1 \to \infty$, the relevant results on the rotating ellipsoidal surface Γ coincide with ones on a sphere.

Theorem 3.1. *The bilinear forms $\hat{D}(\gamma u,\gamma v)$ and $\hat{D}_N(\gamma u,\gamma v)$ in the space $H^{1/2}(\Gamma)$ have the following properties:*
1). Both of two bilinear forms are symmetric;
2). For all $u, v \in H^{1/2}(\Gamma)$, we have

$$|\hat{D}(\gamma u,\gamma v)| \le f_0\cosh\mu_1\|u\|_{H^{1/2}(\Gamma)}\|v\|_{H^{1/2}(\Gamma)},$$
$$|\hat{D}_N(\gamma u,\gamma v)| \le f_0\cosh\mu_1\|u\|_{H^{1/2}(\Gamma)}\|v\|_{H^{1/2}(\Gamma)};$$

3). For all $v \in H^{1/2}(\Gamma)$, we obtain

$$\hat{D}(\gamma v,\gamma v) \ge \hat{D}_N(\gamma v,\gamma v) > \frac{f_0}{4\pi}\sinh\mu_1\left(\int_\Gamma v\mathrm{d}\sigma\right)^2,$$

where $\mathrm{d}\sigma = \sin\theta\mathrm{d}\theta\mathrm{d}\varphi$.

Proof. Obviously, both two bilinear forms are symmetric with respect to u, v. For any u, $v \in H^{1/2}(\Gamma)$, using the definition of the norm in $H^{1/2}(\Gamma)$, the formula (3.4) and Lemma 3.1 yields

$$\begin{aligned}|\hat{D}(\gamma u,\gamma v)| &\le f_0\cosh\mu_1\sum_{n=0}^{\infty}\sum_{m=-n}^{n}(n+1)|V_{nm}^*|\,|U_{nm}|\\ &\le f_0\cosh\mu_1\|u\|_{H^{1/2}(\Gamma)}\|v\|_{H^{1/2}(\Gamma)}.\end{aligned}$$

Using the same inference, we can obtain

$$|\hat{D}_N(\gamma u,\gamma v)| \le f_0\cosh\mu_1\|u\|_{H^{1/2}(\Gamma)}\|v\|_{H^{1/2}(\Gamma)}.$$

$$\begin{aligned}\hat{D}(\gamma v,\gamma v) \geq& \hat{D}_N(\gamma v,\gamma v) = f_0\sum_{n=0}^{N}\sum_{m=-n}^{n} T_{nm}(\mu_1)|V_{nm}|^2\\ \geq& \frac{f_0 T_{00}(\mu_1)}{4\pi}\left(\int_\Gamma v\,d\sigma\right)^2 \geq \frac{f_0\sin\mu_1}{4\pi}\left(\int_\Gamma v\,d\sigma\right)^2.\end{aligned}$$

This completes the proof of the theorem. □

Theorem 3.2. *Suppose that $g\in H^{1/2}(\Gamma_0)$ and $f\in L^2(\Omega_1)$ such that supp$(f)\subset\Omega\cup\Omega_1\cup\Gamma_0$, the variational problems* (3.3) *and* (3.6) *both exist a unique solution. Then we have the following estimates*

$$\begin{aligned}&\|u\|_{H^1(\Omega_1)} \leq C\big(\|f\|_{L^2(\Omega_1)}+\|g\|_{H^{1/2}(\Gamma_0)}\big),\\ &\|u^N\|_{H^1(\Omega_1)} \leq C\big(\|f\|_{L^2(\Omega_1)}+\|g\|_{H^{1/2}(\Gamma_0)}\big).\end{aligned}$$

Proof. From the Trace Theorem, when $g\in H^{1/2}(\Gamma_0)$, there exists $\mathcal{R}g\in H^1(\Omega_1)$ such that $\mathcal{R}g|_{\Gamma_0}=g$ and $\mathcal{R}g|_\Gamma=0$ and

$$\|\mathcal{R}g\|_{H^1(\Omega_1)}\leq C\|g\|_{H^{1/2}(\Gamma_0)}.$$

Let $u_1=u-\mathcal{R}g$ and $u_1^N=u^N-\mathcal{R}g$. Then the equivalent variational problems with the problems (3.3) and (3.6) are respectively: Find $u_1\in V_0(\Omega_1)$ such that

$$D_1(u_1,v)+\hat{D}(\gamma u_1,\gamma v)=\int_{\Omega_1}(f+\Delta\mathcal{R}g)\,v\,d\mathbf{x},\quad \forall\, v\in V_0(\Omega_1), \tag{3.12}$$

and find $u_1^N\in V_0(\Omega_1)$ such that

$$D_1(u_1^N,v)+\hat{D}_N(\gamma u_1^N,\gamma v)=\int_{\Omega_1}(f+\Delta\mathcal{R}g)\,v\,d\mathbf{x},\quad \forall\, v\in V_0(\Omega_1). \tag{3.13}$$

It is obvious that $D_1(\cdot,\cdot)+\hat{D}(\cdot,\cdot)$ and $D_1(\cdot,\cdot)+\hat{D}_N(\cdot,\cdot)$ are both bilinear and symmetric. Theorem 3.1 and the Friedrichs Inequality indicate that there exists a positive constant α such that for any $w\in H^1(\Omega_1)$

$$D_1(w,w)+\hat{D}_N(\gamma w,\gamma w)\geq\int_{\Omega_1}|\nabla w|^2\,d\mathbf{x}+\frac{f_0\sinh\mu_1}{4\pi}\left(\int_\Gamma w\,d\sigma\right)^2\geq\alpha\|w\|_{H^1(\Omega_1)}.$$

For the same reason, we have

$$D_1(w,w)+\hat{D}(\gamma w,\gamma w)\geq\alpha\|w\|^2_{H^1(\Omega_1)}.$$

For any $w,v\in H^1(\Omega_1)$, Theorem 3.1 and the Trace Theorem satisfy

$$\begin{aligned}|D_1(w,v)+\hat{D}(\gamma w,\gamma v)| \leq& |D_1(w,v)|+C_1\|w\|_{H^{1/2}(\Gamma)}\|v\|_{H^{1/2}(\Gamma)}\\ \leq& C\|w\|_{H^1(\Omega_1)}\|v\|_{H^1(\Omega_1)},\\ |D_1(w,v)+\hat{D}_N(\gamma w,\gamma v)| \leq& |D_1(w,v)|+C_1\|w\|_{H^{1/2}(\Gamma)}\|v\|_{H^{1/2}(\Gamma)}\\ \leq& C\|w\|_{H^1(\Omega_1)}\|v\|_{H^1(\Omega_1)}.\end{aligned}$$

Moreover, it follows from $f+\Delta\mathcal{R}g\in H^{-1}(\Omega_1)$ that $\int_{\Omega_1}(f+\Delta\mathcal{R}g)v\mathrm{d}\mathbf{x}$ is a bounded linear functional with respect to v in $H^1(\Omega_1)$. Using the Lax-Milgram Theorem, we know that the problem (3.12) has a unique solution and

$$\begin{aligned}\|u_1\|^2_{H^1(\Omega_1)} \leq & C\int_{\Omega_1}(f+\Delta\mathcal{R}g)\,u_1\,d\mathbf{x} = C\int_{\Omega_1}(f\,u_1+\nabla\mathcal{R}g\cdot\nabla u_1)\,d\mathbf{x}\\ \leq & C\big(\|f\|_{L^2(\Omega_1)}+\|\mathcal{R}g\|_{H^1(\Omega_1)}\big)\|u_1\|_{H^1(\Omega_1)}.\end{aligned}$$

which implies that

$$\|u_1\|_{H^1(\Omega_1)} \leq C\big(\|f\|_{L^2(\Omega_1)}+\|\mathcal{R}g\|_{H^1(\Omega_1)}\big).$$

Therefore, the problem (3.3) exists a unique solution and we have

$$\|u\|_{H^1(\Omega_1)} \leq C\big(\|f\|_{L^2(\Omega_1)}+\|\mathcal{R}g\|_{H^1(\Omega_1)}\big) \leq C\big(\|f\|_{L^2(\Omega_1)}+\|g\|_{H^{1/2}(\Gamma_0)}\big).$$

For the similar reason, the problem (3.6) exists a unique solution and

$$\|u^N\|_{H^1(\Omega_1)} \leq C\big(\|f\|_{L^2(\Omega_1)}+\|g\|_{H^{1/2}(\Gamma_0)}\big). \qquad \square$$

Assume that $\Gamma_1\subset\Omega_1$ is the confocal ellipsoid of Γ and its rotating ellipsoidal coordinate is $(\mu_2,\theta,\varphi)(\mu_2<\mu_1)$. Γ_1 divided the domain Ω_1 into two non-overlapped subdomain Ω_{10} and Ω_{11} such that $\mathrm{supp}(f)\subset\Omega\cup\Omega_{10}\cup\Gamma_0$.

Theorem 3.3. *Suppose that u and u^N are the solutions of the problem* (3.3) *and* (3.6)*, respectively. If $u\in H^{3/2}(\Gamma_1)$, then there is a positive constant C independent of truncation term N such that*

$$\|u-u^N\|_{H^1(\Omega_1)} \leq \frac{C}{N+2}\left(\frac{\cosh\mu_2}{\cosh\mu_1}\right)^{N+2}\|u\|_{H^{3/2}(\Gamma_1)}.$$

Proof. The variational problems (3.3) and (3.6) indicate that

$$D_1(u-u^N,v)+\hat{D}(\gamma u,\gamma v)-\hat{D}_N(\gamma u^N,\gamma v)=0,\quad \forall\, v\in V_0(\Omega_1).$$

Let

$$F_{nm}=\int_\Gamma(u-u^N)|_\Gamma Y^*_{nm}(\theta,\varphi)\,d\sigma,\quad U_{nm}=\int_\Gamma u|_\Gamma Y^*_{nm}\,d\sigma,\quad P_{nm}=\int_{\Gamma_1}u|_{\Gamma_1}Y^*_{nm}\,d\sigma.$$

Then

$$\begin{aligned}&\alpha\|u-u^N\|^2_{H^1(\Omega_1)} \leq D_1(u-u^N,u-u^N)+\hat{D}_N\big(\gamma(u-u^N),\gamma(u-u^N)\big)\\ =&\,\hat{D}_N\big(\gamma u,\gamma(u-u^N)\big)-\hat{D}\big(\gamma u,\gamma(u-u^N)\big)=f_0\sum_{n=N+1}^{\infty}\sum_{m=-n}^{n}T_{nm}(\mu_1)F_{nm}U^*_{nm}\\ \leq&\, f_0\cosh\mu_1\Big(\sum_{n=N+1}^{\infty}\sum_{m=-n}^{n}(n+1)|U_{nm}|^2\Big)^{1/2}\Big(\sum_{n=N+1}^{\infty}\sum_{m=-n}^{n}(n+1)|F_{nm}|^2\Big)^{1/2}\\ \leq&\, f_0\cosh\mu_1\|u-u^N\|_{H^{1/2}(\Gamma)}\Big(\sum_{n=N+1}^{\infty}\sum_{m=-n}^{n}(n+1)|U_{nm}|^2\Big)^{1/2}\\ \leq&\, f_0\cosh\mu_1\,C_{tr}\|u-u^N\|_{H^1(\Omega_1)}\Big(\sum_{n=N+1}^{\infty}\sum_{m=-n}^{n}(n+1)|U_{nm}|^2\Big)^{1/2}.\end{aligned}$$

Set $C = f_0 \cosh\mu_1\, C_{tr}/\alpha$ (independent of N). The formulas (2.4) and (2.10) satisfy

$$U_{nm} = Q_{nm}(\mu_2, \mu_1) P_{nm}.$$

Thus, we have

$$\begin{aligned}\|u - u^N\|^2_{H^1(\Omega_1)} \le & C\Big(\sum_{n=N+1}^{\infty}\sum_{m=-n}^{n}(n+1)|U_{nm}|^2\Big)^{1/2}\\ \le & \frac{C}{N+2}\Big(\sum_{n=N+1}^{\infty}\sum_{m=-n}^{n}(n+1)^3 Q^2_{nm}(\mu_1,\mu)|P_{nm}|^2\Big)^{1/2}\\ \le & \frac{C}{N+2}\Big(\frac{\cosh\mu_2}{\cosh\mu_1}\Big)^{N+2}\|u\|_{H^{3/2}(\Gamma_1)}.\end{aligned}$$

This completes the proof of the theorem. □

4. Discrete Variational Problem and Its Error Estimate

We divide Ω_1 into the regularly quasi-uniformly tetrahedral meshes. When computing the element of the coupled matrix from the bilinear form $\hat{D}_N(\gamma u, \gamma v)$, we adopt the surface triangular elements which are the projections on Γ of the triangles of the tetrahedrons near Γ. Let $V_h(\Omega_1)$ denote the corresponding piecewise linear finite element space on Ω_1 and $\mathcal{N}_h$ be the node set in $\Omega_1 \cup \Gamma_0 \cup \Gamma_1$. Let

$$\begin{aligned}V_g^h(\Omega_1) &= \big\{\, v \in V_h(\Omega_1) : v(\mathbf{a}) = g(\mathbf{a}), \mathbf{a} \in \mathcal{N}_h \cap \Gamma_0 \big\}.\\ V_0^h(\Omega_1) &= \big\{\, v \in V_h(\Omega_1) : v(\mathbf{a}) = 0, \mathbf{a} \in \mathcal{N}_h \cap \Gamma_0 \big\}.\end{aligned}$$

Thus, $V_0^h(\Omega_1) \subset V_0(\Omega_1)$.

The discrete variational problems of the problem (3.3) and (3.6) are the following, respectively: Find $u^h \in V_g^h(\Omega_1)$ such that

$$D_1(u^h, v) + \hat{D}(\gamma u^h, \gamma v) = \int_{\Omega_1} f\, v\, d\mathbf{x}, \quad \forall\, v \in V_0^h(\Omega_1), \tag{4.1}$$

and find $u^{Nh} \in V_g^h(\Omega_1)$ such that

$$D_1(u^{Nh}, v) + \hat{D}(\gamma u^{Nh}, \gamma v) = \int_{\Omega_1} f\, v\, d\mathbf{x}, \quad \forall\, v \in V_0^h(\Omega_1). \tag{4.2}$$

Since $V_0^h(\Omega_1) \subset V_0(\Omega_1)$, the Lax-Milgram Theorem assures that the problems (4.1) and (4.2) are both well-posed.

In the following, we discuss error estimates. Suppose that the linear interpolation operator $\Pi_h : V_g(\Omega_1) \cap H^2(\Omega_1) \mapsto V_g^h(\Omega_1)$ has error estimate

$$|v - \Pi_h v|_{H^s(\Omega_1)} \le C h^{2-s} |v|_{H^2(\Omega_1)}, \quad s = 0, 1.$$

Theorem 4.1. *Assume that $f \in L^2(\Omega_1)$ and $g \in H^{1/2}(\Gamma_0)$. Also let u and u^{Nh} be the solutions of the problem* (3.3) *and* (4.2), *respectively. If $u \in H^2(\Omega_1)$ and $u|_{\Gamma_1} \in H^{3/2}(\Gamma_1)$, then there is a positive constant C independent of the mesh size h and truncation term N such that*

$$\|u - u^{Nh}\|_{H^1(\Omega_1)} \leq C\bigg(h\|u\|_{H^2(\Omega_1)} + \frac{1}{N+2}\left(\frac{\cosh\mu_2}{\cosh\mu_1}\right)^{N+2}\|u\|_{H^{3/2}(\Gamma_1)}\bigg). \tag{4.3}$$

Proof. Let u^N be the solution of the problem (3.6), then

$$D_1(u^N - u^{Nh}, v^h) + \hat{D}_N\big(\gamma(u^N - u^{Nh}), \gamma v^h\big) = 0, \quad \forall\, v^h \in V_0^h(\Omega_1). \tag{4.4}$$

For any $w^h \in V_g^h(\Omega_1)$, $w^h - u^{Nh} \in V_0^h(\Omega_1)$ satisfies

$$\begin{aligned}\alpha\|u^N - u^{Nh}\|^2_{H^1(\Omega_1)} \leq& D_1(u^N - u^{Nh}, u^N - u^{Nh}) + \hat{D}_N\big(\gamma(u^N - u^{Nh}), \gamma(u^N - u^{Nh})\big)\\ =& D_1(u^N - u^{Nh}, u^N - w^h) + \hat{D}_N\big(\gamma(u^N - u^{Nh}), \gamma(u^N - w^h)\big)\\ \leq& C_1\|u^N - u^{Nh}\|_{H^1(\Omega_1)}\|u^N - w^h\|_{H^1(\Omega_1)},\end{aligned}$$

which yields

$$\|u^N - u^{Nh}\|_{H^1(\Omega_1)} \leq \frac{C_1}{\alpha}\|u^N - w^h\|_{H^1(\Omega_1)}, \quad \forall\, w^h \in V_g^h(\Omega_1), \tag{4.5}$$

where C_1 and α are only independent of the domain Ω_1. Thus,

$$\begin{aligned}\|u - u^{Nh}\|_{H^1(\Omega_1)} \leq& \|u - u^N\|_{H^1(\Omega_1)} + \|u^N - u^{Nh}\|_{H^1(\Omega_1)}\\ \leq& \|u - u^N\|_{H^1(\Omega_1)} + \frac{C_1}{\alpha}\|u^N - \Pi_h u\|_{H^1(\Omega_1)}\\ \leq& \Big(1 + \frac{C_1}{\alpha}\Big)\|u - u^N\|_{H^1(\Omega_1)} + \frac{C_1}{\alpha}\|u - \Pi_h u\|_{H^1(\Omega_1)}\\ \leq& \frac{C_1}{\alpha}h\|u\|_{H^2(\Omega_1)} + \Big(1 + \frac{C_1}{\alpha}\Big)\|u - u^N\|_{H^1(\Omega_1)}.\end{aligned}$$

Through Theorem 3.3, we have the formula (4.3). □

Theorem 4.2. *Under the same assumptions of Theorem* 4.1, *there is a positive constant C independent of the mesh size h and the truncation term N such that*

$$\|u - u^{Nh}\|_{L^2(\Omega_1)} \leq C\bigg(h^{\alpha+1}\|u\|_{H^2(\Omega_1)} + \frac{1}{N+2}\left(\frac{\cosh\mu_2}{\cosh\mu_1}\right)^{N+2}\|u\|_{H^{3/2}(\Gamma_1)}\bigg). \tag{4.6}$$

Here, $\alpha > 0$ only depends on the regularity hypothesis of the solution of the problem (2.1).

Proof. Assume that u^N is the solution of the problem (3.6) and $w_1 \in V_0(\Omega_1)$ is the solution to the following problem

$$D_1(v, w_1) + \hat{D}_N(\gamma v, \gamma w_1) = \int_{\Omega_1}(u^N - u^{Nh})v\, d\mathbf{x}, \quad \forall\, v \in V_0(\Omega_1).$$

It can be verified that w_1 has the following regularity hypothesis

$$\|w_1\|_{H^{\alpha+1}(\Omega_1)} \leq C\|u^N - u^{Nh}\|_{L^2(\Omega_1)}, \quad \alpha > 0.$$

Because $\Pi_h w_1 \in V_0^h(\Omega_1)$, the formulas (4.4) and (4.5) imply that

$$\begin{aligned}
&\|u^N - u^{Nh}\|^2_{L^2(\Omega_1)}\\
=& D_1(u^N - u^{Nh}, w_1) + \hat{D}_N\big(\gamma(u^N - u^{Nh}), \gamma w_1\big)\\
=& D_1(u^N - u^{Nh}, w_1 - \Pi_h w_1) + \hat{D}_N\big(\gamma(u^N - u^{Nh}), \gamma(w_1 - \Pi_h w_1)\big)\\
\le& C_1\|w_1 - \Pi_h w_1\|_{H^1(\Omega_1)} \|u^N - u^{Nh}\|_{H^1(\Omega_1)}\\
\le& Ch^\alpha\|w_1\|_{H^{\alpha+1}(\Omega_1)}\|u^N - \Pi_h u\|_{H^1(\Omega_1)}\\
\le& Ch^\alpha \|u^N - u^{Nh}\|_{L^2(\Omega_1)}\big(\|u - \Pi_h u\|_{H^1(\Omega_1)} + \|u - u^N\|_{H^1(\Omega_1)}\big).
\end{aligned}$$

Consequently,

$$\|u^N - u^{Nh}\|_{L^2(\Omega_1)} \le C\left(h^{\alpha+1}\|u\|_{H^2(\Omega_1)} + \frac{h^\alpha}{N+2}\left(\frac{\cosh\mu_2}{\cosh\mu_1}\right)^{N+2}\|u\|_{H^{3/2}(\Gamma_1)}\right).$$

Therefore, we have

$$\begin{aligned}
\|u - u^{Nh}\|_{L^2(\Omega_1)} \le& \|u - u^N\|_{L^2(\Omega_1)} + \|u^N - u^{Nh}\|_{L^2(\Omega_1)}\\
\le& \|u - u^N\|_{H^1(\Omega_1)} + \|u^N - u^{Nh}\|_{L^2(\Omega_1)}\\
\le& C\left(h^{\alpha+1}\|u\|_{H^2(\Omega_1)} + \frac{1}{N+2}\left(\frac{\cosh\mu_2}{\cosh\mu_1}\right)^{N+2}\|u\|_{H^{3/2}(\Gamma_1)}\right).
\end{aligned}$$

This completes the proof of the theorem. □

Remark 4.1. The above estimates indicate that when the mesh size h is given, we choose the optimal truncation term $N_{opt} = \ln(h)/\ln(\cosh\mu_2/\cosh\mu_1) - 2$ with respect to the norm in H^1 and the optimal truncation term $N_{opt} = (\alpha+1)\ln(h)/\ln(\cosh\mu_2/\cosh\mu_1) - 2$ with respect to the norm in L^2.

5. Numerical Examples

Let N denote the truncation term, *nodes* denote the total number of nodes in Ω_1, *tetra* denote the total number of tetrahedral elements in Ω_1. Let

$$\|v\|_0 = \|v\|_{L^2(\Omega_1)}, \quad \|v\|_1 = \|v\|_{H^1(\Omega_1)}, \quad \|v\|_\infty = \|v\|_{L^\infty(\Omega_1)}.$$

In Fig. 5.6 and Fig. 5.11, *Error* denotes the value of $u^{Nh} - u^{50h}$ about three norms when the grid is given. In the other figures, *Error* denotes the value of $u - u^{Nh}$ about the corresponding norms.

Example 5.1. Let $f = 0$, $f_0 = 4$ and the prolate ellipsoid surface $\Gamma_0 = \{(\mu,\theta,\varphi) : \mu = \mu_0, \theta \in [0,\pi], \varphi \in [0, 2\pi)\}$. Assume that the exact solution of the problem (2.1) is

$$u = (x_1^2 + x_2^2 + x_3^2)^{-1/2}.$$

Take $g = u|_{\Gamma_0}$. We choose the prolate ellipsoidal surface $\Gamma = \big\{(\mu,\theta,\varphi) : \mu = \mu_1, \theta \in [0,\pi], \varphi \in [0, 2\pi)\big\}$ as the artificial boundary. $\mu_0 = 0.5$ and $\mu_1 = 1.0$. The correspondent numerical results are shown in Table 5.1 and Fig. 5.1. E_k on axis ordinate of Fig. 5.1 denotes $\|u - u^{Nh}\|_k, k = 0, 1$.

Table 5.1: Example 5.1 Prolate ellipsoid and $N = 50$.

nodes	*tetra*	h	$\parallel u - u^{Nh} \parallel_1$	*ratio*	$\parallel u - u^{Nh} \parallel_0$	*ratio*	$\parallel u - u^{Nh} \parallel_\infty$	*ratio*
52	144	2.7317	1.8815e-1	—	1.2350e-1	—	2.3038e-2	—
342	1344	1.2974	7.1476e-2	2.6324	3.1364e-2	2.0660	5.9223e-3	3.9903
2410	11520	0.6340	3.0187e-2	2.3678	7.8214e-3	4.0100	1.4851e-3	3.9878
17874	95232	0.3135	1.4612e-2	2.0660	1.9601e-3	3.9903	3.6214e-4	4.1009

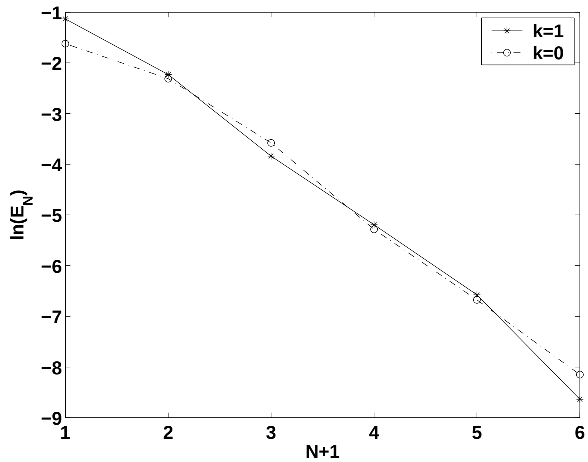

Fig. 5.1. Example 5.1: Prolate ellipsoid, $h = 0.3135$.

Example 5.2. Let $f = 0$ and Γ_0 be the surface of the cuboid $\Omega = \{ (x_1, x_2, x_3) : |x_1| \leq 1, |x_2| \leq 1, |x_3| \leq 3 \}$. Let the exact solution of the problem (2.1) be

$$u = x_1(x_1^2 + x_2^2 + x_3^2)^{-3/2}.$$

Take $g = u|_{\Gamma_0}$. Because the inner domain is elongated, we choose prolate ellipsoidal surface

$$\Gamma = \left\{ (x_1, x_2, x_3) : \frac{x_1^2}{a^2} + \frac{x_2^2}{a^2} + \frac{x_3^2}{9\,a^2} = 1, \quad a \geq \sqrt{3} \right\}$$

as the artificial boundary. The correspondent numerical results are shown in Table 5.2 and Fig. 5.2–Fig. 5.6.

Example 5.3. Let $f = 0$ and Γ_0 be the surface of the cuboid $\Omega = \{ (x_1, x_2, x_3) : |x_1| \leq 3, |x_2| \leq 3, |x_3| \leq 1 \}$. Let the exact solution of the problem (2.1) is

$$u = x_1(x_1^2 + x_2^2 + x_3^2)^{-3/2}.$$

Take $g = u|_{\Gamma_0}$. According to the shape of inner domain, we choose the oblate ellipsoidal surface

$$\Gamma = \left\{ (x_1, x_2, x_3) : \frac{x_1^2}{9\,a^2} + \frac{x_2^2}{9\,a^2} + \frac{x_3^2}{a^2} = 1, a \geq \sqrt{3} \right\}$$

as artificial boundary. The correspondent numerical results are shown in Table 5.3 and Fig. 5.7–5.11.

Table 5.2: Example 5.2: Prolate ellipsoid, $a = 2$ and $N = 50$.

nodes	*tetra*	h	$\parallel u - u^{Nh} \parallel_1$	*ratio*	$\parallel u - u^{Nh} \parallel_0$	*ratio*	$\parallel u - u^{Nh} \parallel_\infty$	*ratio*
232	1008	1.2599	2.4874e-1	—	6.4101e-2	—	3.5785e-2	—
1582	8064	0.7368	1.0120e-1	2.4579	2.8031e-2	2.2868	1.3578e-2	2.6355
11674	64512	0.3889	3.2943e-2	3.0720	9.8109e-3	2.8572	6.5498e-3	2.0730
38342	217728	0.2622	1.5400e-2	2.1390	4.4389e-3	2.2102	2.66328e-3	2.4593

Table 5.3: Example 5.3: Oblate ellipsoid $a = 2$ and $N = 50$.

nodes	*tetra*	h	$\parallel u - u^{Nh} \parallel_1$	*ratio*	$\parallel u - u^{Nh} \parallel_0$	*ratio*	$\parallel u - u^{Nh} \parallel_\infty$	*ratio*
488	2160	1.3896	2.4189e-1	—	8.5921e-2	—	4.7080e-2	—
3374	17280	0.7612	8.3443e-2	2.8988	2.9324e-2	2.9301	1.5732e-2	2.9926
24986	138240	0.3924	2.4973e-2	3.3414	8.6189e-3	3.4023	4.28392e-3	3.6724

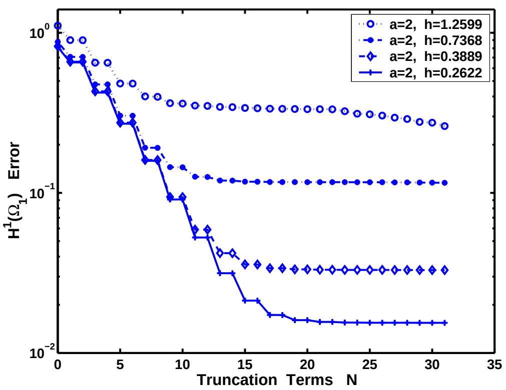

Fig. 5.2. Example 5.2: Relation between h, N and error in $H^1(\Omega_1)$.

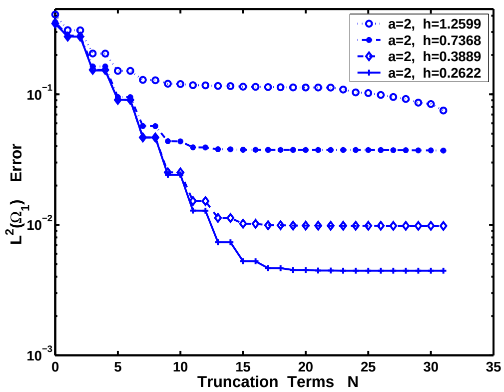

Fig. 5.3. Example 5.2: Relation between h, N and error in $L^2(\Omega_1)$.

6. Conclusions

In this paper, we use the artificial boundary method to solve the Poisson equation over three-dimensional unbounded domain. According to the special shape of the obstacles, we choose the different special artificial boundary, e.g., prolate ellipsoid for cigar-shaped obstacles, and oblate ellipsoid for dish-shaped obstacles. We give the exact artificial boundary conditions, present the coupled variational problems, prove the well-posedness of the solutions of the continuous and discrete coupled variational problem, obtain error estimates, and give some numerical examples. We mainly analyze how truncation term, the mesh size and the location of the artificial boundary have affected the numerical solutions in these examples. The numerical results are in good agreement with the theoretical analysis. The corresponding conclusions are as follows:

1). Figs. 5.2, 5.3, 5.7 and 5.8 have demonstrated that for different mesh sizes h, after truncation term N increases to a certain value (concerned with the mesh size h), the error of the approximate solution with respect to the norms in $H^1(\Omega_1)$ and $L^2(\Omega_1)$ changes very little. This indicates that errors mainly come from the mesh size when the truncation term

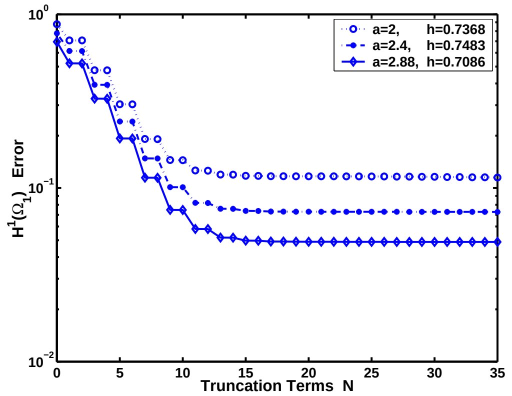

Fig. 5.4. Example 5.2: Relation between location of artificial boundary, N and error in $H^1(\Omega_1)$.

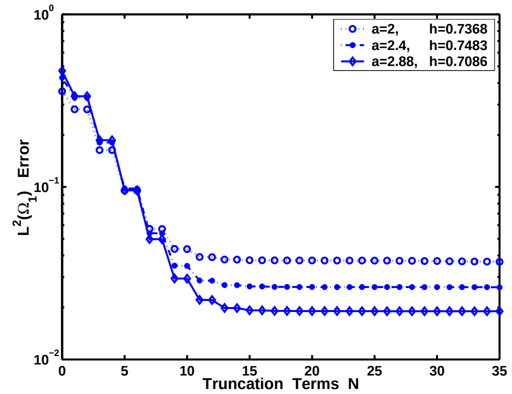

Fig. 5.5. Example 5.2: Relation between location of artificial boundary, N and error in $L^2(\Omega_1)$.

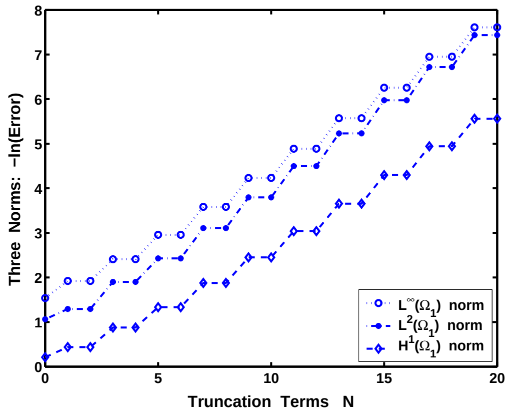

Fig. 5.6. Example 5.2: $h = 0.2622$,$a = 2.0$.

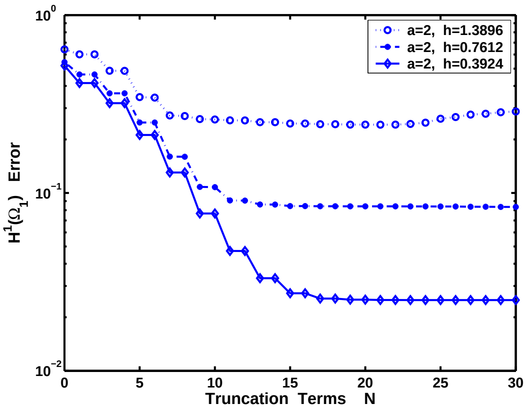

Fig. 5.7. Example 5.3: Relation between mesh, N and error in $H^1(\Omega_1)$.

amounts to a certain value.

2). Tables 5.1– 5.3 have indicated that when truncation term arrive at a certain value, e.g., $N = 50$, the convergent order of $||u - u^{Nh}||_{H^1(\Omega_1)}$ with respect to h is approximate 1, while the convergent order of $||u - u^{Nh}||_{L^\infty(\Omega_1)}$, and $||u - u^{Nh}||_{L^2(\Omega_1)}$ with respect to h is greater than 1.5.

3). Figs. 5.4, 5.5, 5.9 and 5.10 have shown that when h and N are given, the error of the approximate solution become smaller as the distance between Γ_0 and the artificial boundary Γ increase. However, in order to decrease the error, it is inadvisable to extend the distance between Γ_0 and Γ, because if the size of the computational domain is increased, then the computational complexity will increase significantly.

4). Figs. 5.1, 5.6 and 5.11 have illustrated that when the mesh size is given, the relation between the logarithm of the error of $u^{Nh} - u^{50h}$ with respect to three norms and truncation term N is approximately a straight line. This implies that the error of the approximate solution

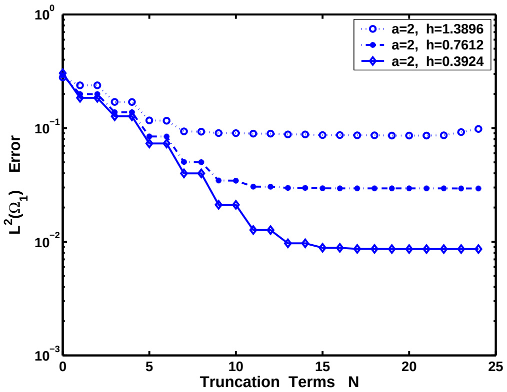

Fig. 5.8. Example 5.3: Relation between mesh, N and error in $L^2(\Omega_1)$.

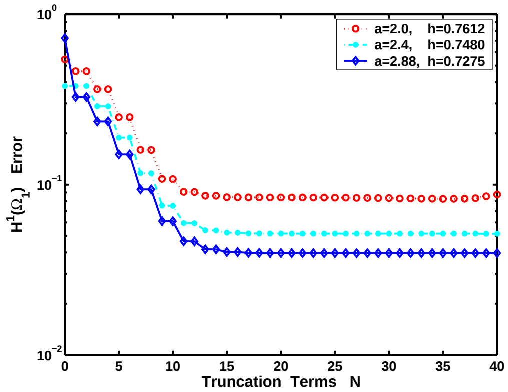

Fig. 5.9. Example 5.3: Relation between location of artificial boundary, N and error in $H^1(\Omega_1)$.

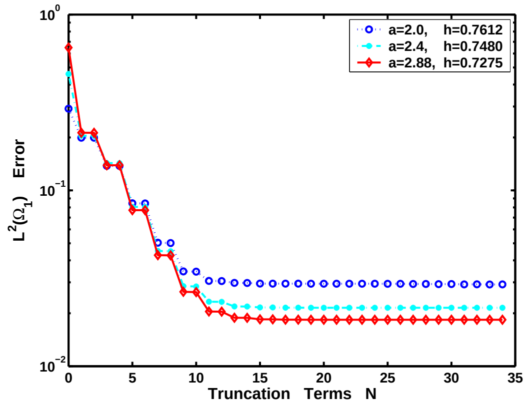

Fig. 5.10. Example 5.3: Relation between location of artificial boundary, N and error in $L^2(\Omega_1)$.

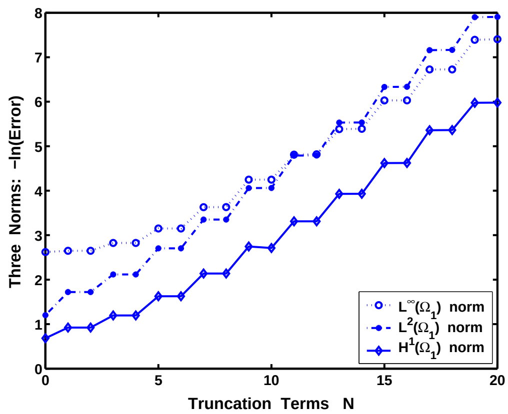

Fig. 5.11. Example 5.3: $h = 0.3924$, $a = 2.0$.

from truncation term is approximately an exponential function about N whose base is less than 1, which is consistent with our theoretic prediction.

Acknowledgment. This work was subsidized by the National Basic Research Program of China under the grant 2005CB321701,the National Natural Science Foundation of China under the grant 10531080, the Beijing Natural Science Foundation under the grant 1072009 and the Research Project of Zhejiang Ocean University (X08M013, X08Z04).

References

[1] M. Abramowitz, I. Stegun, Handbook of Mathematical Function, New York: Dover, 1972.
[2] R.A. Adams, Sobolev Spaces, Academic Press, New York, 1975.
[3] K.J. Bathe and E.L. Wilson, Numerical Methods in Finite Element Analysis, Prentice-Hall, Englewood Cliffs, New York, 1976.
[4] P. Bettess, Infinite elements, *Int. J. Numer. Meth. Eng.*, **11** (1977), 53-64.

[5] C. A. Brebbia, The Boundary Element Method for Engineers, Pentech Press, London, 1978.

[6] F. Brezzi and C. Johnson, On the coupling of boundary integral and finite element methods, *Calcolo*, **76** (1979), 189-201.

[7] P.G. Ciarlet, The Finite Element Method for Elliptic Problems, North-Holland Publishing Company, New York, 1978.

[8] Q.K. Du, D.H. Yu, The coupled method based on natural boundary reduction for parabolic equation, *Comput. Phys.*, **17**:6 (2000), 593-601 (in Chinese).

[9] Q.K. Du, D.H. Yu, On the natural integral equation for initial boundary value problems of two dimensional hyperbolic equation, *Acta Math. Sin.*, **24**:1 (2001), 17-26.

[10] B. Engquist and A. Majda, Absorbing boundary conditions for the numerical simulation of waves, *Math. Comput.*, **31** (1977), 629-651.

[11] D.J. Evans, Numerical solution of exterior problems by the peripheral block overrelaxation method, *J. Inst. Maths. Appl.*, **19** (1977), 399-405.

[12] K. Feng, Differential versus integral equation and finite versus infinite element, *Mathematicae Numerica Sinica*, **2**:1 (1980), 100-105.

[13] K. Feng, D.H. Yu, Canonical integral equations of elliptic boundary value problems and their numerical solutions, In Proceedings of China-France Symposium on Finite Element Method, Beijing: Science Press, 1983, 211-252.

[14] C.I. Goldstein, A finite element method for solving Helmholtz type equations in waveguides and other unbounded domains, *Math. Comput.*, **39**:160 (1982), 309-324.

[15] T.M. Hagstrom and H.B. Keller, Exact boundary conditions at artificial boundary for partial differential equations in cylinders, *SIAM J. Math. Anal.*, **17** (1986), 322-341.

[16] T.M. Hagstrom and H.B. Keller, Asymptotic boundary conditions and numerical methods for nonlinear elliptic problems on unbounded domains, *Math. Comput.*, **48** (1987), 449-470.

[17] H.D. Han, X.N. Wu, Approximation of infinite boundary condition and its application to finite element methods, *J. Comput. Math.*, **3**:3 (1985), 179-192.

[18] H.D. Han, A new class of variational formulations for the coupling of finite and boundary element methods, *J. Comput. Math.*, **8** (1990), 223-232.

[19] H.D. Han and X.N. Wu, The approximation of the exact boundary conditions at an artificial boundary for linear elastic equations and its application, *Math. Comput.*, **59** (1992), 21-37.

[20] H.D. Han, W.Z. Bao, Error estimates for the finite element approximation of problems in unbounded domains, *SIAM J. Numer. Anal.*, **37** (2000), 1101-1119.

[21] Q.Y. Hu and D.H. Yu, A solution method for a certain nonlinear interface problem in unbounded domains, *Computing*, **67** (2001), 119-140.

[22] H.Y. Huang and D.H. Yu, Natural boundary element method for three dimensional exterior harmonic problem with an inner prolate spheroid boundary, *J. Comput. Math.*, **24**:2 (2006), 193-208.

[23] H.Y. Huang and D.H. Yu, The coupled NBEM and FEM for three-dimensional exterior problem with a prolate spherical artificial boundary, In Proceedings of the Fourth International Workshop on Scientific Computing and Applications, Beijing: Science Press, 2007, 117-122.

[24] H.Y. Huang, An Artificial Boundary Method for Three-Dimensional Problems over Unbounded Domain with an Ellipsoidal Artificial Boundary, PhD Dissertation, Academy of Mathematics and System Sciences of the Chinese Academy of Sciences, 2007 (in Chinese).

[25] C. Johnson and J.C. Nedelec, On the coupling of boundary integral and finite element methods, *Math. Comput.*, **35** (1980), 1063-1079.

[26] J.B. Keller, M.J. Grote, Exact non-reflecting boundary conditions, *J. Comput. Phys.*, **82** (1989), 172-192.

[27] J.B. Keller, M.J. Grote, On non-reflecting boundary conditions, *J. Comput. Phys.*, **122** (1995), 231-243.

[28] Y. Liu, Solution of Some Electromagnetic Problems Based on Natural Boundary Elements and Domain Decomposition Method, PhD Dissertation, Academy of Mathematics and System Sciences

of the Chinese Academy of Sciences, 2007 (in Chinese).

[29] J.M. Wu, Natural Boundary Element Method and Domain Decomposition Algorithm for Three Dimensional Problems, PhD Dissertation, Institute of Computational Mathematics, the Chinese Academy of Sciences, 1999 (in Chinese).

[30] D.H. Yu, Coupling canonical boundary element method with FEM to solve harmonic problem over cracked domain, *J. Comput. Math.*, **1**:3 (1983), 195-202.

[31] D.H. Yu, Approximation of boundary conditions at infinity for a harmonic equation, *J. Comput. Math.*, **3**:3 (1985), 219-227.

[32] D.H. Yu, Natural Boundary Integral Method and its Applications, Dordrecht, Netherlands:Kluwer Academic Publishers, 2002.

[33] J.L. Zhu, Boundary Element Analysis of Elliptic Boundary Value Problems, Beijing: Science Press, 1992 (in Chinese).

[34] O.C. Zienkiewicz, D.W. Kelly, and P. Bettess, The coupling of the finite element method and boundary solution procedures, *Int. J. Numer. Meth. Eng.*, **11** (1977), 355-375.

[35] M. Costabel, E.P. Stephan, Coupling of finite element and boundary element methods for an elasto-plastic interface problems, *SIAM Numer. Anal.*, **27** (1990), 1212-1226.

[36] G.N. Gatica, L.F. Gatica, E.P. Stephan, A FEM-DtN formulation for a nonlinear exterior problem in incompressible elasticity, *Math. Method. Appl. Sci.*, **26** (2003), 151-170.